Supporting Information
A strategy for modulating the catalytic active center of AP thermal decomposition and its application: La-doped $MgCo_2O_4$

Guofei Zhang [a], Xin Yu [a], Zhenlong Wang [a], Sirong Li [a], Zhengyi Zhao [a], Yunjiong Zhu [a], Yude Wang [b*], Xuechun Xiao [a*]

a *School of Materials and Energy, Yunnan University, 650091 Kunming, People's Republic of China*

b *Yunnan Key Laboratory of Carbon Neutrality and Green Low-carbon Technologies, Yunnan University, 650091 Kunming, People's Republic of China*

* To whom correspondence should be addressed. Tel: +86-871-65037399, Fax: +86-871-65153832. E-mail: ydwang@ynu.edu.cn (Y. D. Wang)

* To whom correspondence should be addressed. Tel: +86-871-65037399, Fax: +86-871-65153832. E-mail: xchxiao@ynu.edu.cn (X. CH. Xiao)

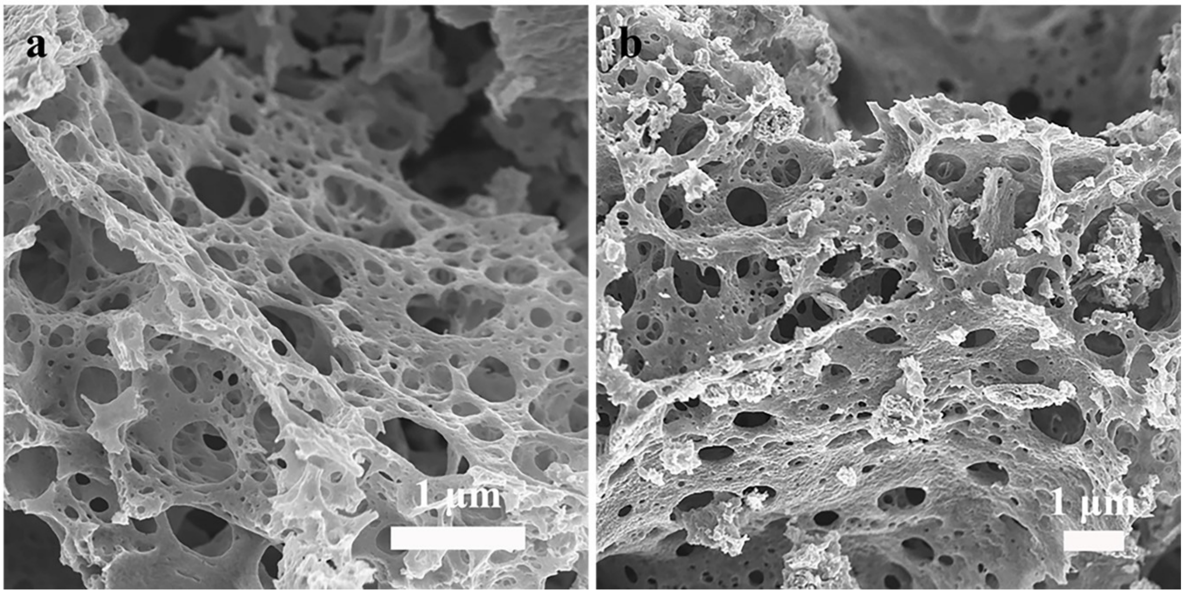

Fig. S1 The SEM patterns of the as-prepared Lax-$MgCo_2O_4$: (a) x=0.75%, (b) x=2%.

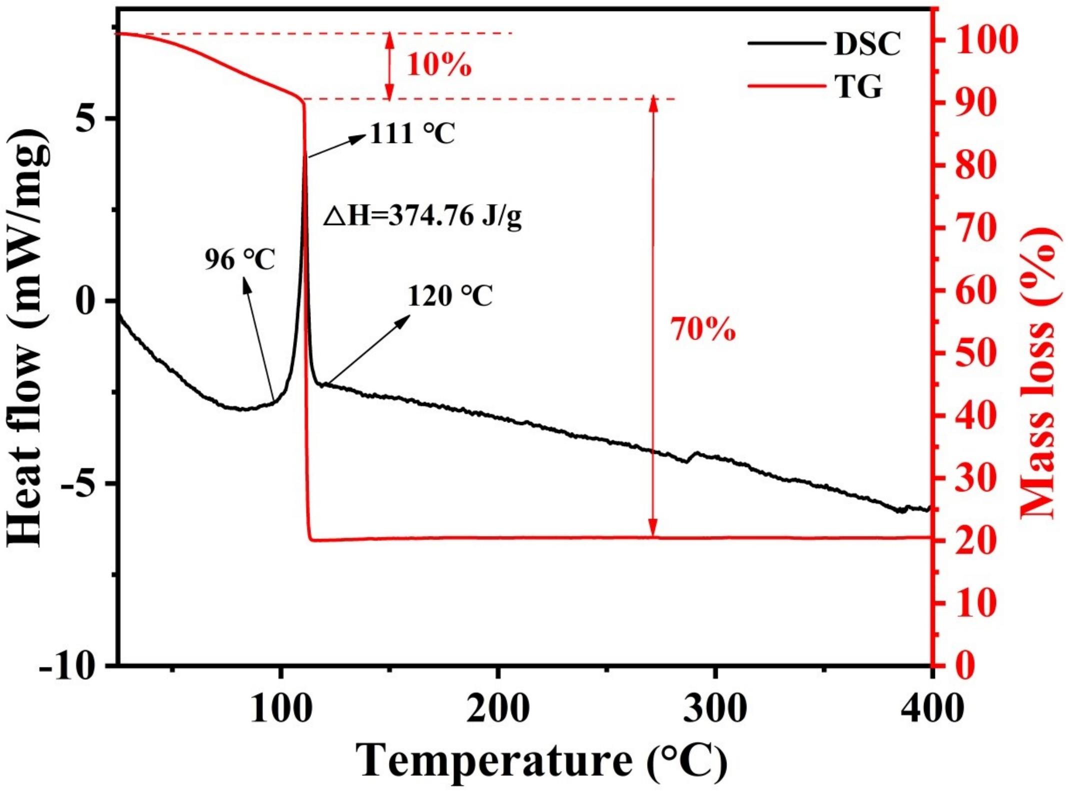

Fig. S2 TG-DSC curve of La1%-$MgCo_2O_4$ precursors (Heating rate 5°C/min, holding at 400°C for 1h).

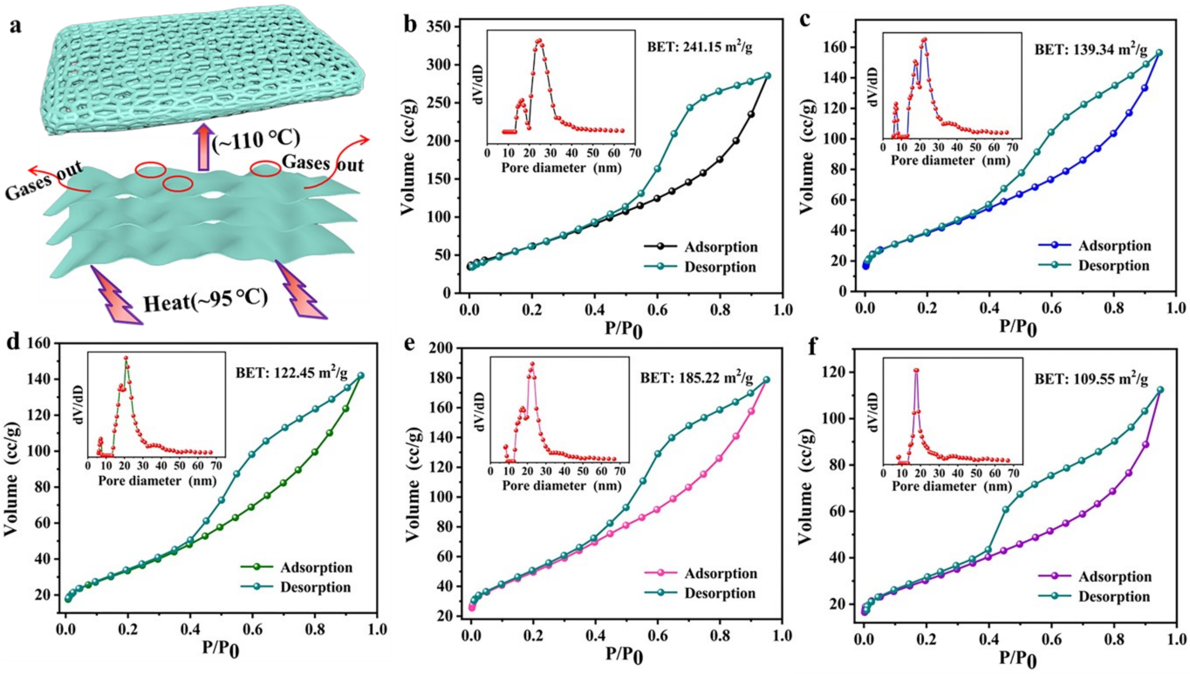

Fig. S3 (a) The formation process of Lax-$MgCo_2O_4$ porous structure; Nitrogen adsorption-desorption isotherm of the as-synthesized (b) Pure $MgCo_2O_4$, (c)La0.5%-$MgCo_2O_4$, (b) La0.75%-$MgCo_2O_4$, (c) La1%-$MgCo_2O_4$ and (d) La2%-$MgCo_2O_4$, respectively. Insert is the pore-size distribution calculated by the DFT method from desorption branch of the Lax-$MgCo_2O_4$, respectively.

Table S1 The structural parameters and BET specific surface area of pure $MgCo_2O_4$ and La_x-$MgCo_2O_4$ (x = 0.5%, 0.75%, 1%, 2%).

Samples	DFT pore size (nm)	DFT pore volume (cm^3/g)	BET specific surface area (m^2/g)
La2%-$MgCo_2O_4$	18.14	0.64	109.55
La1%-$MgCo_2O_4$	21.71	1.02	185.22
La0.75%-$MgCo_2O_4$	20.76	0.81	122.45
La0.5%-$MgCo_2O_4$	22.71	0.89	139.34
$MgCo_2O_4$	16.57	1.62	241.15

Table S2 The relative ratios of O_{Latt}, O_V and -OH in O 1s of the pure $MgCo_2O_4$ and Lax-$MgCo_2O_4$ (x = 0.5%, 0.75%, 1%, 2%).

Samples	O_{Latt} relative content (%)	O_V relative content (%)	-OH relative content (%)
La2%-$MgCo_2O_4$	47.31	35.16	17.53
La1%-$MgCo_2O_4$	43.17	43.96	12.87
La0.75%-$MgCo_2O_4$	46.08	41.02	12.90
$MgCo_2O_4$	43.15	40.84	16.01

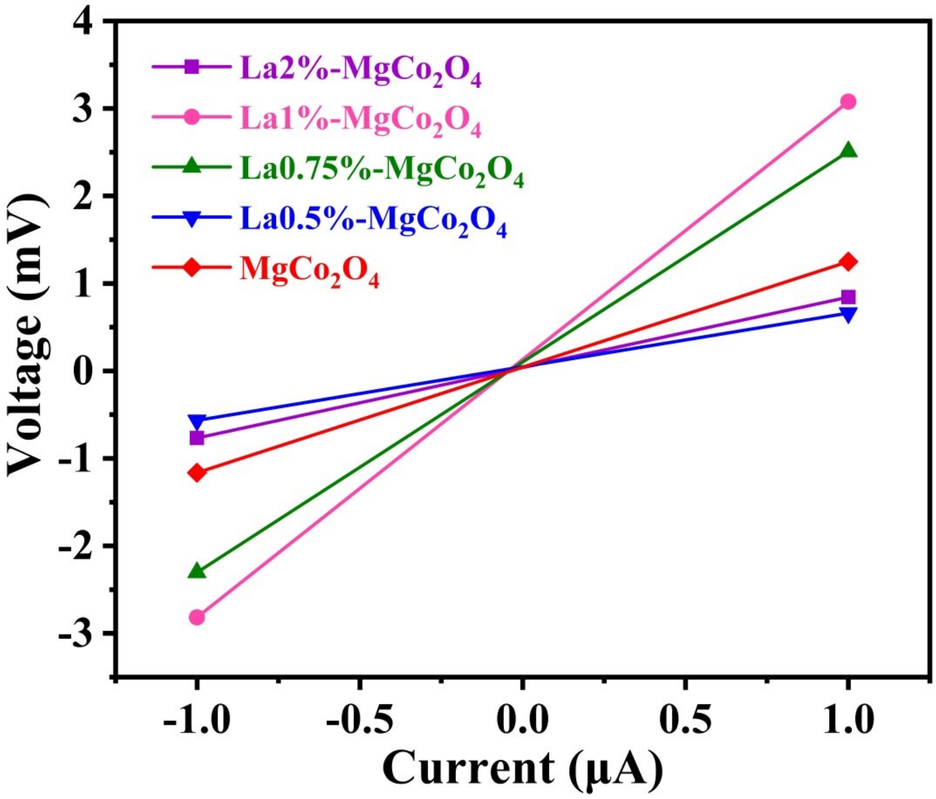

Fig. S4 Current-voltage curve of pure $MgCo_2O_4$ and Lax-$MgCo_2O_4$ (x=0.5%, 0.75%, 1% and 2%).

Table S3 The carrier concentration and P/N type of pure $MgCo_2O_4$ and Lax-$MgCo_2O_4$ (x=0.5%, 0.75%, 1% and 2%).

Samples	Hall coefficient ($cm^3 \cdot c^{-1}$)	Resistvity (ohm·cm)	Carrier concentration (cm^{-3})	P/N type
La2%-$MgCo_2O_4$	3.62×10^2	28.87	3.40×10^{16}	P
La1%-$MgCo_2O_4$	3.13×10^1	28.24	1.99×10^{17}	P
La0.75%-$MgCo_2O_4$	1.04×10^2	30.02	8.43×10^{16}	P
La0.5%-$MgCo_2O_4$	1.50×10^2	30.41	4.17×10^{16}	P
$MgCo_2O_4$	1.69×10^2	121.46	3.68×10^{16}	P

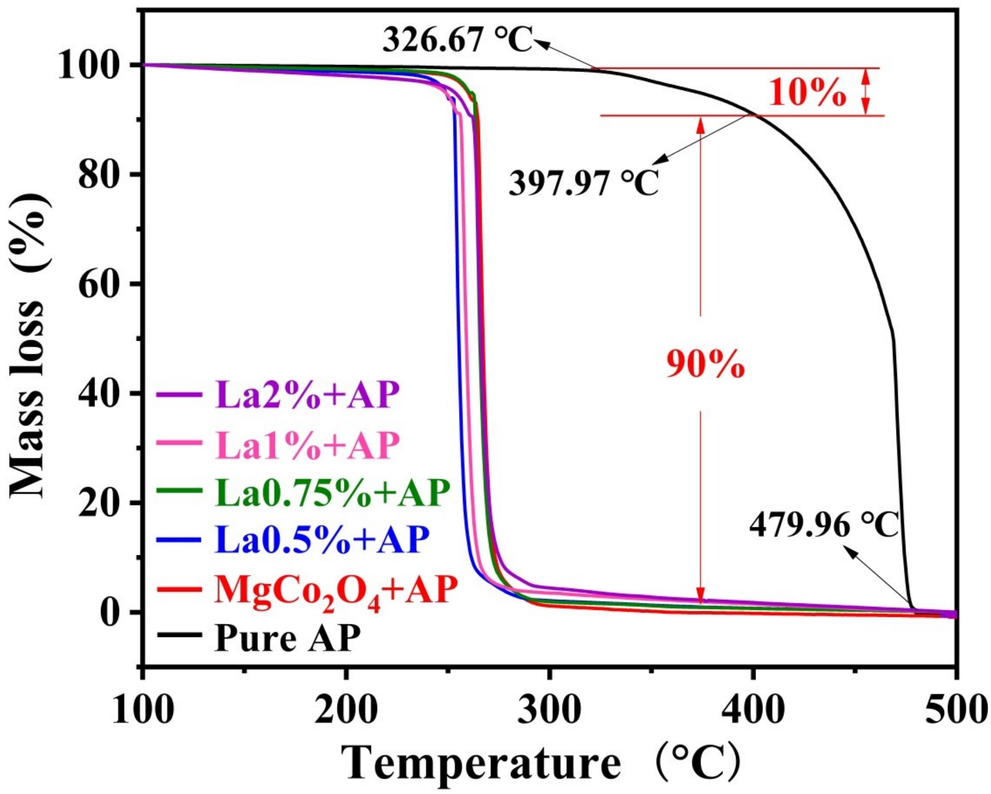

Fig. S5 TG curves of the AP thermal decomposition with and without pure $MgCo_2O_4$ and Lax-$MgCo_2O_4$ (x=0.5%, 0.75%, 1% and 2%).

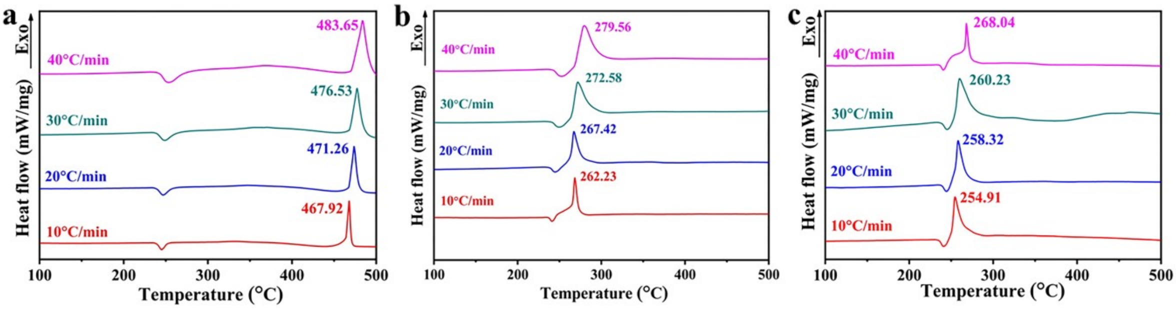

Fig. S6 DSC curves at the different heating rate (10, 20, 30, 40 °C·min^{-1}): (a) Pure AP, (b) 2% pure $MgCo_2O_4$ + AP, (c) 2%La1%-$MgCo_2O_4$ + AP, respectively.

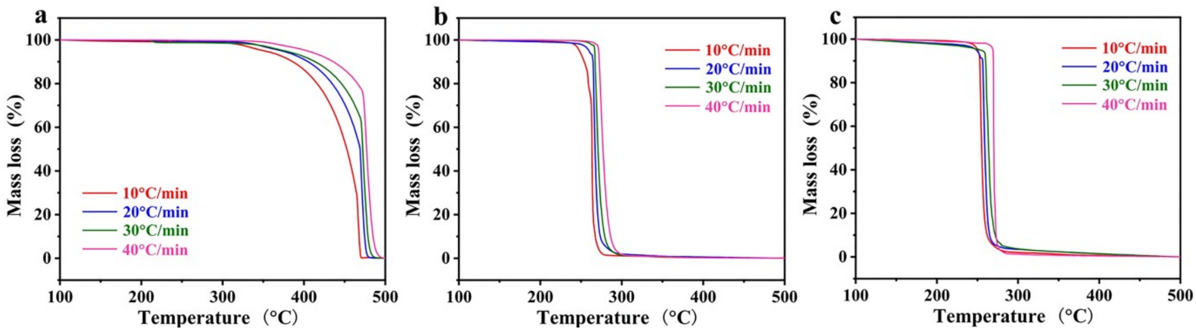

Fig. S7 TG curves at the different heating rate (10, 20, 30, 40 °C·min^{-1}): (a) Pure AP, (b) 2% pure $MgCo_2O_4$ + AP, (c) 2%La1%-$MgCo_2O_4$ + AP, respectively.

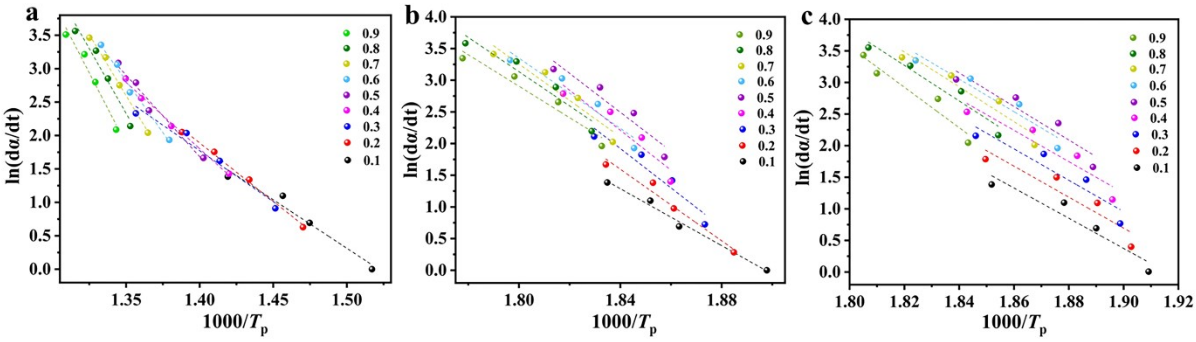

Fig. S8 Linear fit curve to TG analysis using Friedman method (α increments of 0.1): (a) Pure AP, (b) 2% pure $MgCo_2O_4$ + AP, (c) 2%La1%-$MgCo_2O_4$ + AP, respectively.

Table S4 TG kinetic results calculated by Friedman method.

Conversion (α)	Friedman method (E_{aF}, kJ·mol^{-1})		
	Pure AP	2%$MgCo_2O_4$ + AP	2%La1%-$MgCo_2O_4$ + AP
0.1	199.54	166.28	157.98
0.2	221.38	186.81	160.02
0.3	228.81	188.89	161.29
0.4	236.42	190.25	162.95
0.5	249.76	191.46	161.87
0.6	272.13	180.68	165.46
0.7	284.64	188.52	170.43
0.8	295.87	181.99	178.75
0.9	300.28	184.56	187.07

Table S5 Comparison of catalytic activity of AP by various catalysts.

Samples	M %	β °C·min^{-1}	Decrease of T_{HTD} (°C)	Decrease of E_a (kJ·mol^{-1})	Increase of k (s^{-1})	Refs.
Flower-like Ni	3	10	70.00	-	-	[52]
Nanosheets Co_3O_4	2	20	132.30	57.9	-	[11]
3DOM Fe_2O_3/Co_3O_4	1	20	49.94	61.1	-	[17]
Co_3O_4@MnO_2	2	10	112.00	-	-	[53]
Nanoparticles $CoFe_2O_4$	3	20	89.50	16.15	0.08	[54]
Hollow $NiCo_2O_4$	1	20	49.94	-	-	[18]
Nano $FeCo_2O_4$	2	20	196.25	93.70	1.20	[27]
MXene/$ZnCo_2O_4$	2	20	132.00	111.7	-	[55]
Nanosheets La1%-$MgCo_2O_4$	2	20	215.16	120.39	3.62	This work

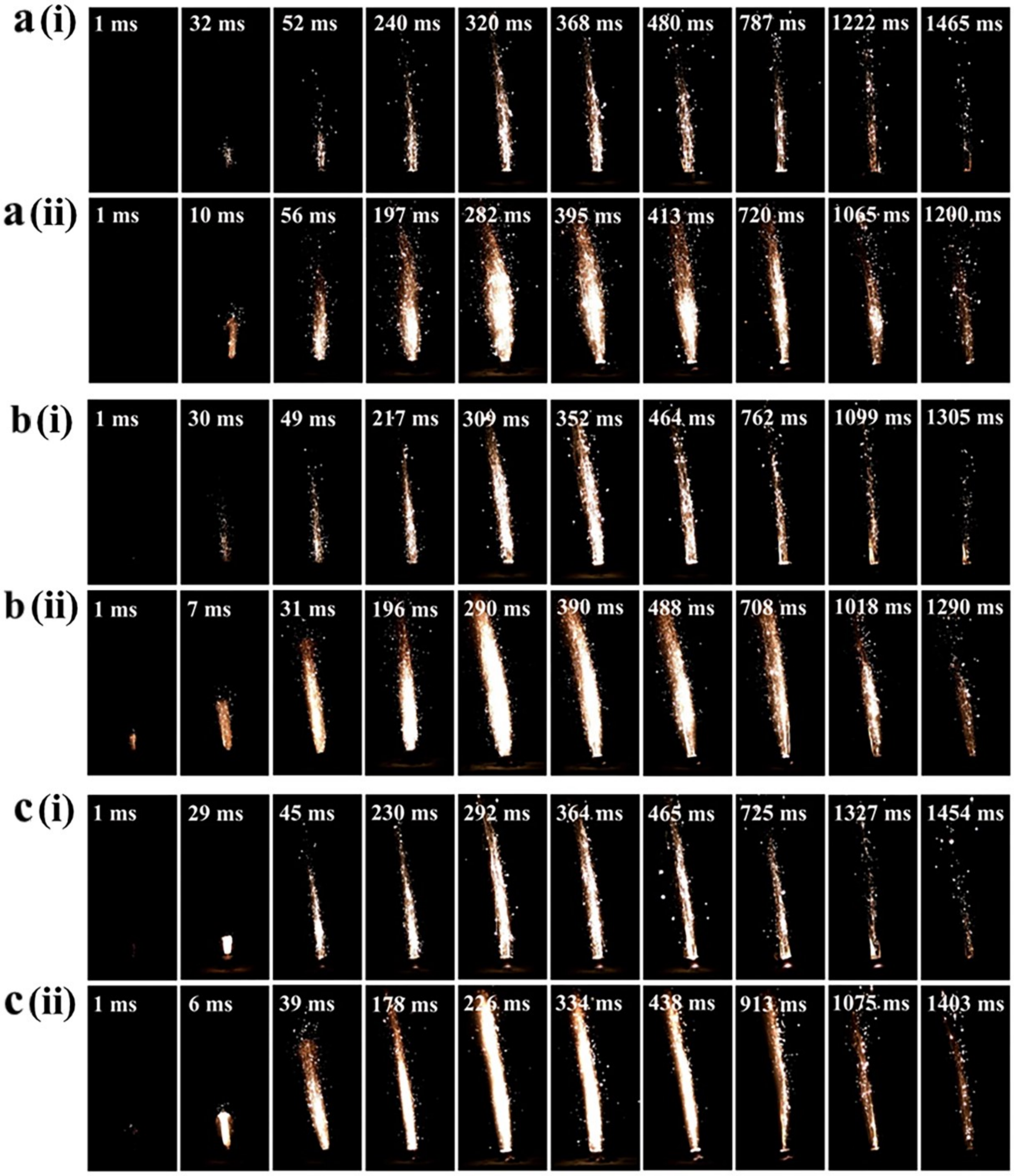

Fig. S9 Laser ignited combustion of (a(i)) AP/HTPB, (a(ii)) La1%-$MgCo_2O_4$-AP/HTPB (Ignition voltage is 22 V); (b(i)) AP/HTPB, (b(ii)) La1%-$MgCo_2O_4$-AP/HTPB (Ignition voltage is 34 V); (c(i)) AP/HTPB, (c(ii)) La1%-$MgCo_2O_4$-AP/HTPB (Ignition voltage is 46 V).